Available online at www.sciencedirect.com
SCIENCE DIRECT®
Journal of Organometallic Chemistry 689 (2004) 2464–2472
Journal of Organometallic Chemistry
www.elsevier.com/locate/jorganchem

[1,1′-Bis(diphenylphosphino)ferrocene]palladium(II) complexes with fluorinated benzenethiolate ligands: examination of the electronic effects in the solid state, solution and in the Pd-catalyzed Heck reaction with the catalytic system $[Pd(dppf)(SR_F)_2]$ ☆

César Herrera-Álvarez [a], Valente Gómez-Benítez [a], Rocío Redón [b], Juventino J. García [c], Simón Hernández-Ortega [a], Rubén A. Toscano [a], David Morales-Morales [a,*]

[a] *Instituto de Química, Universidad Nacional Autónoma de México, Cd. Universitaria, Circuito Exterior, Coyoacán, 04510 México City DF, México*
[b] *Centro de Ciencias Aplicadas y Desarrollo Tecnológico (CCADET), Universidad Nacional Autónoma de México, Cd. Universitaria, Circuito Exterior, Coyoacán, 04510 México City DF, México*
[c] *Facultad de Química, 04510 México City DF, México*

Received 11 March 2004; accepted 29 April 2004

Abstract

A series of palladium thiolate complexes of the type $[Pd(dppf)(SR_F)_2]$ have been synthesized in good yields by metathetical reactions of $[Pd(dppf)Cl_2]$ with $[Pb(SR_F)_2]$, ($SR_F = {}^-SC_6F_5$, ${}^-SC_6F_4$-4-H, ${}^-SC_6H_4$-2-CF_3, ${}^-SC_6H_4$-4-F, ${}^-SC_6H_4$-3-F) and their crystal structures determined. The effect of the different thiolates in the structural properties of the complexes both in the solid state and in solution have been analyzed. Heck coupling reactions were carried out using the complexes $[Pd(dppf)(SR_F)_2]$, $SR_F = {}^-SC_6F_5$ (**1**), ${}^-SC_6F_4$-4-H (**2**), ${}^-SC_6H_4$-2-CF_3 (**3**), ${}^-SC_6H_4$-4-F (**4**), ${}^-SC_6H_4$-3-F (**5**) as catalysts in order to examine both the effect of the thiolates and the P–Pd–P bite angles in the reaction of bromobenzene and styrene. The results obtained indicate that electron-withdrawing substituents may favor higher yields in the Pd catalyzed Heck reaction using $[Pd(dppf)(SR_F)_2]$ as catalysts.

Keywords: Heck reaction; dppf; C–C coupling reactions; Fluorinated thiolate complexes; Palladium complexes; Crystal structures; Catalysis

1. Introduction

Since 1,1′-bis(diphenylphosphino)ferrocene (dppf) was first synthesized by Bishop et al. in 1971 [1], this compound has been employed profusely for the synthesis of complexes otherwise difficult or in some cases almost impossible to isolate with other diphosphines (e.g., dppe) [2]. In recent years, this capability of stabilization, has been applied to the synthesis of species with potential applications in homogeneous catalysis [3]. This is particularly true in the case of C–C coupling reactions [4]. Thus, the high interest in these transformations has led different research groups to the design and synthesis of alternative ferrocene based ligands, including chiral inductors [5]. In addition, platinum group metal complexes containing ferrocene and thiolate ligands on its structure are rare [6], due in part to the well known tendency of these complexes to polymerize [7], affording in most of the cases intractable solids useless as potential catalysts in homogeneous catalysis. Moreover, compounds containing sulfur on its structure have been left out from its possible applications as homogeneous catalysts due to the extended believe of sulfur as a catalyst poison. Thus, given our continuous interest in the design and synthesis of active and robust complexes for employment as potential catalysts in

☆ Supplementary data associated with this article can be found, in the online version, at doi:10.1016/j.jorganchem.2004.04.035.

* Corresponding author. Tel.: +52-555-622-4514; fax: +52-555-616-2217.
E-mail address: damor@servidor.unam.mx (D. Morales-Morales).

0022-328X/$ - see front matter © 2004 Elsevier B.V. All rights reserved.
doi:10.1016/j.jorganchem.2004.04.035

industrial relevant transformations [8], we would like to report here the use of dppf as a stabilizing ligand and fluorinated thiolates as substituents for the fine tuning of the electronics in the synthesis of a series of palladium(II) complexes of the type $[Pd(dppf)(SR_F)_2]$. The identification of the electronic effects of the different fluorinated thiolates over the physical properties, structure and reactivity in catalytic Heck reaction experiments will be discussed.

2. Results and discussion

The reaction of one equivalent of the lead salt of the corresponding thiolate $[Pb(SR_F)_2]$ with one equivalent of $[Pd(dppf)(Cl)_2]$ afford complexes **1**–**5** in good yields. All compounds were obtained as analytically pure products from recrystallization of CH_2Cl_2/MeOH solvent systems. Given the similarity in the structures of these complexes, common features in their spectroscopic properties exist. The information obtained from ^1H NMR of the series of complexes is not very informative since only common signals due to the presence of the aromatics and the cyclopentadienyl (Cp) rings in the dppf moiety are observed. The $^{31}P\{^1H\}$ NMR spectra of the compounds are more illustrative affording in all cases single resonances indicative of magnetic equivalence of the P nuclei in the coordinated dppf moiety. Another important feature in these spectra is that the signals observed are sensitive, as expected, to the number and position of fluorine atoms in the aromatic ring. Thus, in the case of $[Pd(dppf)(SC_6F_5)_2]$ (**1**) the signal is shifted to lower field ($\delta = 28.16$ ppm) and in the case of $[Pd(dppf)(SC_6H_4\text{-}2\text{-}CF_3)_2]$ (**3**) the signal is displaced to higher field ($\delta = 25.22$ ppm); these two examples represent the upper and lower limits in the series of complexes. This behavior can be rationalized from the point of view of electron-withdrawing capability, being higher in the case of complex **1** due the higher substitution of fluorine of the aromatic ring, and therefore, with the larger value of Group Electronegativity (Eg) [9], having as the ultimate consequence the deshielding of the P nuclei in the dppf moiety. Thus, the trend observed for the δ $^{31}P\{^1H\}$ in the series of complexes $[Pd(dppf)(SR_F)_2]$ is $^-SC_6H_4\text{-}2\text{-}CF_3$ (25.22 ppm) < $^-SC_6H_4\text{-}3\text{-}F$ (25.55 ppm) < $^-SC_6H_4\text{-}4\text{-}F$ (26.21 ppm) < $^-SC_6F_4\text{-}4\text{-}H$ (27.65 ppm) < $^-SC_6F_5$ (28.16 ppm).

On the other hand, the $^{19}F\{^1H\}$ NMR experiments of the synthesized complexes reveal the fluorinated thiolates to be present, with typical splitting patterns for the ligands $^-SC_6F_5$ (**1**) and $^-SC_6F_4\text{-}4\text{-}H$ (**2**) and singlets for the cases $^-SC_6H_4\text{-}2\text{-}CF_3$ (**3**), $^-SC_6H_4\text{-}4\text{-}F$ (**4**), $^-SC_6H_4\text{-}3\text{-}F$ (**5**). These observed patterns are in agreement with the proposed formulations. Additionally, analysis by FAB^+-Mass spectrometry shows in all cases the molecular ion of the fragment corresponding to the loss of one thiolate ligand. Further loss of the other thiolate ligand and a diphenylphosphine fragment from the dppf ligand were also observed. Elemental analyses for all the complexes are consistent with the proposed formulations.

Crystals suitable for single crystal X-ray diffraction analysis (Table 1) were obtained for all the complexes in the series, once again these compounds share a number of common structural features. The structures can be defined as slightly distorted square planar in all cases, having the palladium centers with the dppf ligand coordinated in a bidentate manner and completing the coordination sphere with the two thiolates adopting a *cis* conformation, each *trans* to one phosphorus of the dppf ligand. The main distortion is due to the steric hindrance caused by the phenyl rings in the dppf ligand. In all cases, the aromatic rings of the thiolates are not eclipsed as has been observed in other cases due to π–π interactions [10]. Instead, the aromatic rings are shifted, in an *anti* configuration. It is probable that the fluorobenzene rings adopt this conformation due to steric hindrance or to have optimal packing in the lattice.

The differences observed, particularly in the $^{31}P\{^1H\}$ NMR experiments, are complemented with the results obtained from single crystal X-ray diffraction experiments. Here, the differences in changing the thiolates are very clear. For instance, the Pd–S bond lengths (Table 2) increase as the value of the Eg increases in the following order: $^-SC_6H_4\text{-}4\text{-}F$ (2.34 Å) < $^-SC_6F_4\text{-}4\text{-}H$ (2.35 Å) < $^-SC_6F_5$ (2.36 Å). This is most likely the result of either steric hindrance or electrostatic repulsion phenomena. Furthermore, it has been noticed that depending on the position of the fluorinated substituent on the aromatic ring, the Pd–S bond lengths also vary -$^-SC_6H_4\text{-}2\text{-}CF_3$ (2.37 Å) > $^-SC_6H_4\text{-}3\text{-}F$ (2.35 Å) > $^-SC_6H_4\text{-}4\text{-}F$ (2.34 Å)-, which may be a consequence of steric hindrance or a result of the way the molecules pack in the lattice. An analogous behavior is observed in the case of the Pd–P bond distances, where a similar trend is observed, ($^-SC_6H_4\text{-}2\text{-}CF_3$ (2.314 Å) < $^-SC_6F_4\text{-}4\text{-}H$ (2.316 Å) < $^-SC_6F_5$ (2.317 Å)) however, in this case the trend observed for the probable effect of the position of the substituent in the aromatic ring is the opposite to the case exposed previously -$^-SC_6H_4\text{-}2\text{-}CF_3$ (2.314 Å) = $^-SC_6H_4\text{-}3\text{-}F$ (2.314 Å) > $^-SC_6H_4\text{-}4\text{-}F$ (2.319 Å)-. This fact, may indeed mean that the behavior observed is mainly due to the packing in the lattice more than a real influence due to steric hindrance. Another clear trend can be observed in the values of the S–Pd–S angles, where the smallest angle of the series is observed for complex **1** which contains the thiolate ligand $^-SC_6F_5$ with the higher value of Eg, while the bigger angle corresponds to complex **4** which contains the ligand $^-SC_6H_4\text{-}4\text{-}F$ on its structure. A similar trend is observed for the values of the P–Pd–P angles where the smallest angle (98.41°) is once again

Table 1
Summary of crystal structure data for [Pd(dppf)(SR_F)$_2$] $R_F = C_6F_5$ (**1**), C_6F_4-4-H (**2**), C_6H_4-4-CF_3 (**3**), C_6H_4-4-F (**4**), C_6H_4-3-F (**5**)

Compound	[Pd(dppf)(SC_6F_5)$_2$] (**1**)	[Pd(dppf)(SC_6F_4-4-H)$_2$] (**2**)	[Pd(dppf)(SC_6H_4-2-CF_3)$_2$] (**3**)	[Pd(dppf)(SC_6H_4-4-F)$_2$] (**4**)	[Pd(dppf)(SC_6H_4-3-F)$_2$] (**5**)
Empirical formula	$C_{46}H_{28}F_{10}FeP_2PdS_2$	$C_{46}H_{30}F_8FeP_2PdS_2$	$C_{48}H_{36}F_6FeP_2PdS_2$	$C_{46}H_{36}F_2FeP_2PdS_2$	$C_{46}H_{36}F_2FeP_2PdS_2$
Formula weight	1058.99	1023.01	934.06	915.06	915.06
Temperature (K)	291(2)	291(2)	291(2)	291(2)	291(2)
Crystal system	Monoclinic	Monoclinic	Monoclinic	Monoclinic	Monoclinic
Space group	$P2_1/n$	$P2_1/n$	$C2/c$	$P2_1/n$	$P2_1/n$
Cystal size (mm)	$0.32 \times 0.18 \times 0.04$	$0.41 \times 0.12 \times 0.048$	$0.30 \times 0.14 \times 0.025$	$0.43 \times 0.26 \times 0.018$	$0.35 \times 0.22 \times 0.047$
Unit cell dimensions					
a (Å)	11.1930(5)	10.881(1)	26.683(3)	19.219(1)	10.8854(14)
b (Å)	20.7028(9)	20.632(1)	11.5371(12)	21.834(1)	20.531(2)
c (Å)	18.5164(8)	18.532(1)	15.0307(16)	19.939(1)	18.341(2)
α (°)	90	90	90	90	90
β (°)	94.75	94.52	115.59	108.08	95.79
γ (°)	90	90	90	90	90
Volume (Å^3)	4280.1(3)	4147.5(5)	4173.2(8)	7953.7(6)	4036.8(8)
Z	4	4	4	4	4
Density (g/cm^3)	1.643	1.638	1.487	1.543	1.506
θ Range for data collection	2.05 a 25°	1.97 a 25°	1.69 a 25°	1.42 a 25°	1.98 a 25°
Reflections collected	34 845	33 676	16 600	64 554	7518
Independent reflections	7528 [$R_{int} = 0.087$]	7311 [$R_{int} = 0.07$]	3677 [$R_{int} = 0.11$]	14 025 [$R_{int} = 0.1$]	7115 [$R_{int} = 0.04$]
$F(000)$	2112	2048	1892	1856	3752
Absorption correction	None	Analytic	None	Integration	Analytic
Goodness-of-fit on F^2	0.770	0.984	1.000	1.020	0.984
R indices (all data)	$R_1 = 0.079$, $wR_2 = 0.062$	$R_1 = 0.074$, $wR_2 = 0.055$	$R_1 = 0.053$, $wR_2 = 0.105$	$R_1 = 0.115$, $wR_2 = 0.28$	$R_1 = 0.111$, $wR_2 = 0.070$
Final R indices $[I > 2\sigma(I)]$	$R_1 = 0.042$, $wR_2 = 0.056$	$R_1 = 0.041$, $wR_2 = 0.050$	$R_1 = 0.046$, $wR_2 = 0.102$	$R_1 = 0.058$, $wR_2 = 0.11$	$R_1 = 0.052$, $wR_2 = 0.061$
Data/restrains/ parameters	7528/0/55	7311/0/541	3677/0/272	7115/0/488	14 025/2/988
Index ranges	$-13 \leqslant k \leqslant 13$, $-24 \leqslant h \leqslant 24$, $-22 \leqslant l \leqslant 22$	$-12 \leqslant k \leqslant 12$, $-24 \leqslant h \leqslant 24$, $-22 \leqslant l \leqslant 22$	$-31 \leqslant k \leqslant 31$, $-13 \leqslant h \leqslant 13$, $-17 \leqslant l \leqslant 17$	$0 \leqslant k \leqslant 12$, $0 \leqslant h \leqslant 24$, $-21 \leqslant l \leqslant 21$	$-22 \leqslant k \leqslant 22$, $-25 \leqslant h \leqslant 25$, $-23 \leqslant l \leqslant 23$

* $S = [w(F_o)^2 - (F_c)^2)^2/(n-p)]^{1/2}$ where n = number of reflections and p = total number of parameters.
** $R_1 = |F_o - F_c|/|F_o|$, $wR_2 = [w((F_o)^2 - (F_c)^2)^2/w(F_o)^2]^{1/2}$.

observed for $^-SC_6F_5$ and the larger angle (102.2°) for the compound containing the ligand $^-SC_6H_4$-2-CF_3, with the smallest Eg value (see Table 3).

In 1984, Hayashi first reported the use of the palladium derivative [Pd(dppf)Cl_2] as a superior catalyst in C–C bond coupling reactions [11]. In fact, Gan and Hor [3] have referred to this complex as a magic catalyst. The outstanding reactivity was attributed to its larger P–Pd–P bite angle (99.07°). However, recent studies by Hayashi himself suggest that smaller P–Pd–P bond angles might indeed be more important than larger bite angles [12].

We believe that we have an ideal system to attempt to shed some light in order to discriminate whether larger or smaller P–Pd–P bite angles are important in palladium catalyzed C–C bond forming reactions. Thus, catalytic experiments were carried out employing the complexes [Pd(dppf)(SR_F)$_2$] as catalysts. The reactions of bromobenzene and styrene using *N,N*-dimethylformamide (DMF) as a solvent were carried out in the open air at different reaction times, revealing that 2 h of reaction time would yield enough product (stilbenes) to observe a clear trend to be able to quantify the bite angle effects as well as the effects due to the variation of the Eg of the thiolates. Given the fact that single substituted thiolates in different positions of the aromatic ring were also employed, some insights with respect to the sterics can also be obtained.

To better visualize the above-mentioned effects, graphs of the yield of stilbenes versus P–Pd–P angle (Graphic 1) and the yield of stilbenes versus Eg (Graphic 2) were plotted. From this graphic, one observes that as the bite angle increases the yield of stilbenes decreases, in accordance with the recent observations reported by Hayashi and co-workers [12]. However, in Graphic 1, one point lies out of this line.

Table 2
Selected bond lengths (Å) and angles (°) for [Pd(dppf)(SR_F)$_2$] $R_F = C_6F_5$ (**1**), C_6F_4-4-H (**2**), C_6H_4-4-CF_3 (**3**), C_6H_4-4-F (**4**), C_6H_4-3-F (**5**)

[Pd(dppf)(SC_6F_5)$_2$] (**1**)		[Pd(dppf)(SC_6F_4-4-H)$_2$] (**2**)		[Pd(dppf)(SC_6H_4-2-CF_3)$_2$] (**3**)		[Pd(dppf)(SC_6H_4-4-F)$_2$] (**4**)		[Pd(dppf)(SC_6H_4-3-F)$_2$] (**5**)	
Bond lengths (Å)									
Pd–P(1)	2.2939(8)	Pd–P(1)	2.3064(11)	Pd–P(1)	2.3143(9)	Pd–P(1)	2.3215(16)	Pd–P(1)	2.3128(17)
Pd–P(2)	2.3448(8)	Pd–P(2)	2.3183(11)	Pd–P(1*)	2.3142(9)	Pd–P(2)	2.3168(15)	Pd–P(2)	2.3158(17)
Pd–S(1)	2.3694(8)	Pd–S(1)	2.3519(11)	Pd–S(1)	2.3706(10)	Pd–S(1)	2.3486(15)	Pd–S(1)	2.3338(18)
Pd–S(2)	2.3763(8)	Pd–S(2)	2.3577(10)	Pd–S(1*)	2.3710(10)	Pd–S(2)	2.3363(16)	Pd–S(2)	2.3583(17)
S(1)–C(35)	1.751(4)	S(1)–C(1)	1.749(4)	S(1)–C(18)	1.7470(4)	S(1)–C(1)	1.7330(6)	S(1)–C(41)	1.7580(8)
S(2)–C(41)	1.762(3)	S(2)–C(7)	1.739(4)	S(1*)–C(18*)	1.7400(4)	S(2)–C(7)	1.7540(6)	S(2)–C(35)	1.7620(8)
P(1)–C(6)	1.825(3)	P(1)–C(37)	1.813(4)	P(1)–C(1)	1.8150(4)	P(1)–C(37)	1.7920(6)	P(1)–C(1)	1.8280(7)
P(2)–C(1)	1.817(3)	P(2)–C(42)	1.794(4)	P(1*)–C(1*)	1.8150(4)	P(2)–C(42)	1.8040(5)	P(2)–C(6)	1.7970(8)
P(1)–P(2)	3.463(3)	P(1)–P(2)	3.502(4)	P(1)–P(1*)	3.602(4)	P(1)–P(2)	3.497(5)	P(1)–P(2)	3.517(7)
Bond angles (°)									
S(1)–Pd–S(2)	92.09(3)	S(1)–Pd–S(2)	91.85(4)	S(1)–Pd–S(1*)	93.18	S(1)–Pd–S(2)	95.40(6)	S(1)–Pd–S(2)	92.47(6)
S(1)–Pd–P(1)	174.57(3)	S(1)–Pd–P(1)	167.28(4)	S(1)–Pd–P(1)	84.52	S(1)–Pd–P(1)	81.96(5)	S(1)–Pd–P(1)	166.04(8)
S(2)–Pd–P(1)	84.50(3)	S(2)–Pd–P(1)	83.65(4)	S(1*)–Pd–P(1)	163.46	S(2)–Pd–P(1)	171.48(6)	S(2)–Pd–P(1)	84.90(6)
S(1)–Pd–P(2)	171.31(3)	S(1)–Pd–P(2)	87.14(4)	S(1)–Pd–P(1*)	163.86	S(1)–Pd–P(2)	175.67(6)	S(1)–Pd–P(2)	85.61(6)
S(2)–Pd–P(2)	85.55(3)	S(2)–Pd–P(2)	174.40(4)	S(1*)–Pd–P(1*)	84.52	S(2)–Pd–P(2)	85.36(5)	S(2)–Pd–P(2)	172.70(7)
P(1)–Pd–P(2)	96.58(3)	P(1)–Pd–P(2)	98.46(4)	P(1)–Pd–P(1*)	102.20	P(1)–Pd–P(2)	97.88(5)	P(1)–Pd–P(2)	98.62(6)
P(1)–C(1)–Fe(1)	125.32(16)	P(1)–C(37)–Fe(1)	126.30(19)	P(1)–C(1*)–Fe(1)	122.61	P(1)–C(37)–Fe	127.0(3)	P(1)–C(1)–Fe	125.5(3)
P(2)–C(6)–Fe(1)	119.93(15)	P(2)–C(42)–Fe(1)	121.10(19)	P(1*)–C(1*)–Fe(1)	122.31	P(2)–C(42)–Fe	125.0(3)	P(2)–C(6)–Fe	120.3(4)

It may be possible that this particular complex may not be as stable as the other analogous complexes under the catalytic reaction conditions, which may account for the lowering in yield.

In Graphic 2, yield of stilbenes versus Group Electronegativity (Eg), an inverse behavior is observed, (solid line), in which complex **1** ($^{-}SC_6F_5$ with the highest value of Eg) displays the higher yield of the reaction (21.45%). From this graphic, it is not clear whether the position of the substituent in the aromatic ring of the thiolate plays an important role in the production of stilbenes. Thus, it seems that at least in the present case, the electronics is a more important factor than sterics, however this has to be investigated further employing bigger substituents in the aromatic ring of the thiolate. Moreover, from the graphs it seems that a palladium system containing dppf as a ligand and electron withdrawing substituents may render complexes with smaller bite angles which in turn may lead to an excellent catalyst for the high yield catalyzed Heck reaction.

In summary, we have reported an efficient synthetic procedure for the synthesis of monomeric [Pd(dppf)(SR_F)$_2$] complexes. These compounds have been studied and clear trends can be observed for Eg versus the properties of these species in solution and in the solid state. Preliminary catalytic experiments indicate that complexes containing small P–Pd–P bite angles are more reactive than those with larger P–Pd–P angles. A clear trend is also observed as the value of Eg is varied, indicating that electron-withdrawing substituents may favor higher yields in the Pd catalyzed Heck reaction using [Pd(dppf)(SR_F)$_2$] as the catalytic system. Efforts aimed to employ these compounds in metal mediated organic syntheses and other C–C coupling reactions are currently under investigation.

3. Experimental

3.1. Materials and methods

Unless stated otherwise, all reactions were carried out under an atmosphere of dinitrogen using conventional Schlenk glassware and solvents were dried using established procedures and distilled under dinitrogen immediately prior to use. The IR spectra were recorded on a Nicolet-Magna 750 FT-IR spectrometer as nujol mulls. The ^{1}H NMR (300 MHz) spectra were recorded on a JEOL GX300 spectrometer. Chemical shifts are reported in ppm down field of TMS using the solvent ($CDCl_3$, $\delta = 7.27$) as an internal standard. $^{31}P\{^1H\}$ NMR (121 MHz) and $^{19}F\{^1H\}$ spectra were recorded with complete proton decoupling and are reported in ppm using 85% H_3PO_4 and C_6F_6 as external standards, respectively. Elemental analyses were determined on a

Table 3
Heck couplings of bromobenzene with [Pd(dppf)(SR_F)$_2$] $R_F = C_6F_5$ (**1**), C_6F_4-4-H (**2**), C_6H_4-4-CF_3 (**3**), C_6H_4-4-F (**4**), C_6H_4-3-F (**5**) as catalyst

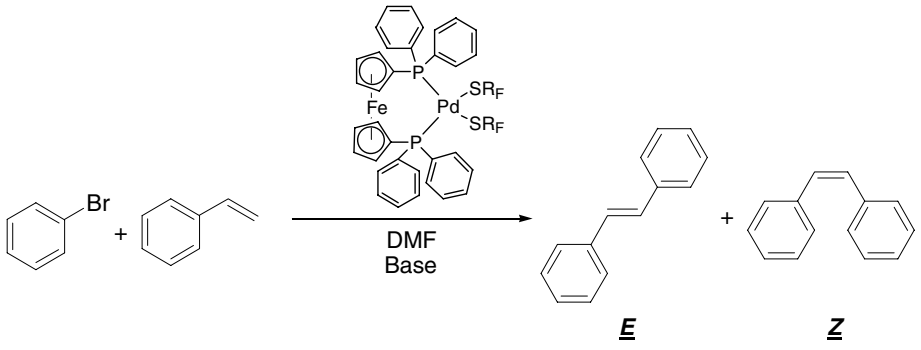

Entry	SR_F	Eg	P–Pd–P angle (°C)	P–Pd bond length[b] (Å)	Conversion[a] (%)
1	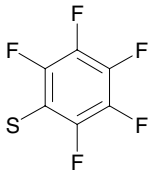	3.07	96.58(3)	2.3194(8)	21.45
2	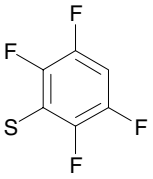	2.92	98.46(4)	2.3124(11)	19.61
3	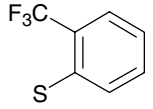	2.48	102.20(5)	2.3143(9)	11.42
4	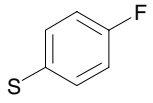	2.48	97.88(5)	2.3192(16)	13.75
5	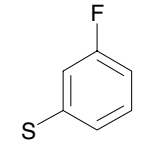	2.48	98.62(6)	2.3143(17)	17.60

Reaction conditions 50 mmol of halobenzene, 60 mmol of styrene, 60 mmol of base, 4.0×10^{-5} mmol of catalyst and 5 ml of DMF, 2 h at 120 °C.
[a] Yields obtained by GC are based on bromobenzene.
[b] Values are the average of the two different values observed for the Pd–P distances.

Perkin–Elmer 240. Positive-ion FAB mass spectra were recorded on a JEOL JMS-SX102A mass spectrometer operated at an accelerating voltage of 10 kv. Samples were desorbed from a nitrobenzyl alcohol (NOBA) matrix using 3 keV xenon atoms. Mass measurements in FAB are performed at a resolution of 3000 using magnetic field scans and the matrix ions as the reference material or, alternatively, by electric field scans with the sample peak bracketed by two (polyethylene glycol or cesium iodide) reference ions. GC–MS quantitative analyses were performed on a Varian Saturn 3 with a 30.0 m DB-5 capillary column.

The 1,1′-bis(diphenylphosphino)ferrocene (dppf) and $PdCl_2$ were obtained commercially from Aldrich Chem. Co. Compounds [Pd(COD)Cl_2] [13], [Pd(dppf)Cl_2] [11] and [Pb(SR_F)$_2$] [14]; $R_F = C_6F_5$, C_6F_4-4-H, C_6H_4-2-

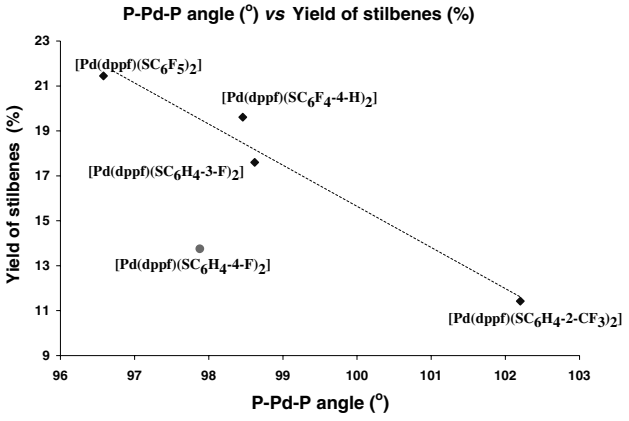

Graphic 1.

CF_3, C_6H_4-4-F, C_6H_4-3-F were synthesized according to the published procedures.

3.2. General procedure for the synthesis of the complexes $[Pd(dppf)(SR_F)_2]$

All the complexes were obtained using the same experimental procedure. As a representative example the synthesis of $[Pd(dppf)(SC_6F_5)_2]$ is described (see Scheme 1).

3.3. Synthesis of $[Pd(dppf)(SC_6F_5)_2]$ (**1**)

To a solution of $[Pd(dppf)(Cl)_2]$ (50.0 mg, 0.068 mmol) in CH_2Cl_2 (10 ml), a solution of $[Pb(SC_6F_5)_2]$ (41.3 mg, 0.068 mmol) in acetone (20 ml) was added dropwise under stirring, the resulting red-brick solution was allowed to stir overnight, after which time the solution was filtered through a short plug of Celite® and the solvent removed under vacuum. The residue was recrystallized from CH_2Cl_2–Hexane, to afford **1** as a deep red microcrystalline powder. Yield 90%. NMR ^1H (300 MHz, $CDCl_3$), δ 7.95–7.25 (*m*, Ph, 20H), 4.43 (*s*, Cp, 4H), 4.27 (*s*, Cp, 4H); NMR $^{31}P\{^1H\}$ (121 MHz, $CDCl_3$), δ 28.16 (s, P); NMR $^{19}F\{^1H\}$ (282 MHz, $CDCl_3$), δ −135.08 (*d*, $^3J_{Fo-Fm} = 22.01$ Hz, *o*-F), −164.56 (*t*, $^3J_{Fm-Fp} = 22.01$ Hz, *p*-F), −166.87 (*m*, $^4J_{Fo-Fp} = 4.79$, *m*-F). Elementary Analalysis Calculated for $[C_{46}H_{28}F_{10}Fe_1P_2Pd_1S_2]$ Calc. (%): C: 52.17, H: 2.66. Found (%): C: 52.14, H: 2.68. MS-FAB$^+$ $[M^+] = 1059$ *m*/*z*.

3.4. Synthesis of $[Pd(dppf)(SC_6F_4\text{-}4\text{-}H)_2]$ (**2**)

$[Pd(dppf)(Cl)_2]$ (50.0 mg, 0.068 mmol) in CH_2Cl_2 (10 ml), a solution of $[Pb(SC_6F_4\text{-}4\text{-}H)_2]$ (39.0 mg, 0.068 mmol) in acetone (20 ml). Yield 83.5%. NMR ^1H (300

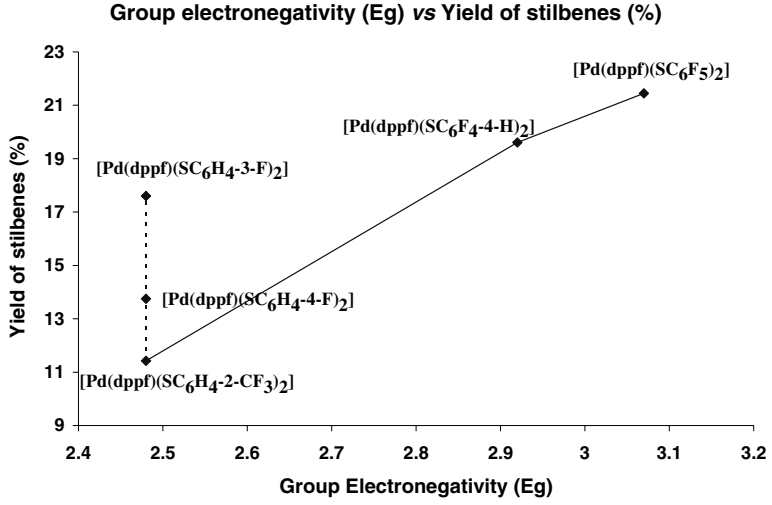

Graphic 2.

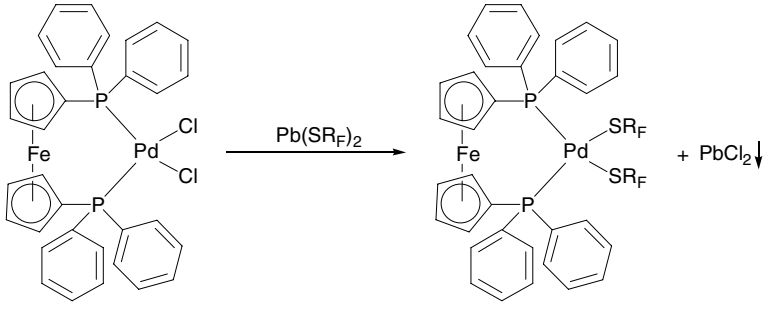

Scheme 1. Metathesis reactions for the synthesis of the complexes $[Pd(dppf)(SR_F)_2]$.

MHz, $CDCl_3$), δ 7.95–7.25 (*m*, Ph, 22H), 4.41 (*s*, Cp, 4H), 4.28 (*s*, Cp, 4H); NMR $^{31}P\{^1H\}$(121 MHz, $CDCl_3$), δ 27.65 (s, P); NMR $^{19}F\{^1H\}$ (282 MHz, $CDCl_3$), δ −135.45 (*m*, $^3J_{Fo–Fm} = 24.27$ Hz, *o*-F), −143.75 (*m*, $^3J_{Fm–Fo} = 24.27$ Hz, *m*-F). Elementary Analysis Calculated for $[C_{46}H_{30}F_8Fe_1P_2Pd_1S_2]$ Calc. %: C: 54.00, H: 2.96. Found %: C: 54.06, H: 2.98. MS-FAB$^+$ $[M^+] = 1022$ *m/z*.

3.5. Synthesis of [Pd(dppf)(SC_6H_4-2-CF_3)$_2$] (3)

$[Pd(dppf)(Cl)_2]$ (50.0 mg, 0.068 mmol) in CH_2Cl_2 (10 ml), a solution of $[Pb(SC_6H_4\text{-}2\text{-}CF_3)_2]$ (38.4 mg, 0.068 mmol) in acetone (20 ml). Yield 76.5%. NMR ^1H (300 MHz, $CDCl_3$), δ 7.98–6.90 (*m*, Ph, 28H), 4.38 (*s*, Cp, 4H), 4.22 (*s*, Cp, 4H); NMR $^{31}P\{^1H\}$ (121 MHz, $CDCl_3$), δ 25.23 (s, P); NMR $^{19}F\{^1H\}$ (282 MHz, $CDCl_3$), δ −61.05 (*s*, CF_3). Elementary Analysis Calculated for $[C_{48}H_{36}F_6Fe_1P_2Pd_1S_2]$ Calc. %: C: 56.79, H: 3.57. Found %: C: 56.76, H: 3.58. MS-FAB$^+$ $[M^+] = 1014$ *m/z*.

3.6. Synthesis of [Pd(dppf)(SC_6H_4-4-F)$_2$] (4)

$[Pd(dppf)(Cl)_2]$ (50.0 mg, 0.068 mmol) in CH_2Cl_2 (10 ml), a solution of $[Pb(SC_6H_4\text{-}4\text{-}F)_2]$ (31.5 mg, 0.068 mmol) in acetone (20 ml). Yield 93.5%. NMR ^1H (300 MHz, $CDCl_3$), δ 7.93–6.98 (*m*, Ph, 28H), 4.39 (*s*, Cp, 4H), 4.20 (*s*, Cp, 4H); NMR $^{31}P\{^1H\}$(121 MHz, $CDCl_3$), δ 26.21 (s, P); NMR $^{19}F\{^1H\}$ (282 MHz, $CDCl_3$), δ −116.33 (*s*, *p*-F). Elementary Analaysis Calculated for $[C_{46}H_{36}F_2Fe_1P_2Pd_1S_2]$ Calc. %: C: 60.37, H: 3.97. Found %: C: 60.34, H: 3.98. MS-FAB$^+$ $[M^+] = 914$ *m/z*.

3.7. Synthesis of [Pd(dppf)(SC_6H_4-3-F)$_2$] (5)

$[Pd(dppf)(Cl)_2]$ (50.0 mg, 0.068 mmol) in CH_2Cl_2 (10 ml), a solution of $[Pb(SC_6H_4\text{-}3\text{-}F)_2]$ (31.5 mg, 0.068 mmol) in acetone (20 ml). Yield 92.8%. NMR ^1H (300 MHz, $CDCl_3$), δ 8.00–6.42 (*m*, Ph, 28H), 4.38 (*s*, Cp, 4H), 4.18 (*s*, Cp, 4H); NMR $^{31}P\{^1H\}$(121 MHz, $CDCl_3$), δ 25.55 (s, P); NMR $^{19}F\{^1H\}$(282 MHz, $CDCl_3$), δ −112.15 (*s*, *m*-F). Elementary Analysis Calculated for $[C_{46}H_{36}F_2Fe_1P_2Pd_1S_2]$ Calc. %: C: 60.37, H: 3.97. Found %: C: 60.36, H: 3.94. MS-FAB$^+$ $[M^+] = 914$ *m/z*.

3.8. General procedure for the catalytic reactions

A DMF solution (5 ml) of 50.0 mmol of bromobenzene, 60.0 mmol of styrene, and the prescribed amount of catalyst was introduced into a Schlenk tube in the open air. The tube was charged with a magnetic stir bar and an equimolar amount of base, sealed, and fully immersed in a 120 °C silicon oil bath. After the prescribed reaction time (2 h), the mixture was cooled to room temperature and the organic phase was analyzed by gas chromatography (GC/FID, GC–MS). A Varian Saturn 3 with DB-5 capillary column (30.0 m) was used for quantitative GC analysis (see Scheme 2).

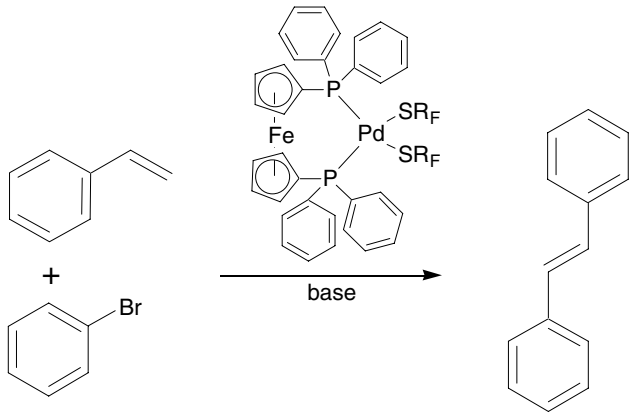

Scheme 2. The palladium catalyzed Heck coupling reaction using $[Pd(dppf)(SR_F)_2]$ as the catalyst.

3.9. Data collection and refinement for [Pd(dppf)(SC_6F_5)$_2$] (1), [Pd(dppf)(SC_6F_4-4-H)$_2$] (2), [Pd(dppf)(SC_6H_4-2-CF_3)$_2$] (3), [Pd(dppf)(SC_6H_4-4-F)$_2$] (4), [Pd(dppf)(SC_6H_4-3-F)$_2$] (5)

Crystalline orange prisms for **1**, **4** and **5** and red-orange prisms for **2** and **3** were grown independently by slow evaporation of CH_2Cl_2/MeOH solvent systems, and mounted on glass fibers. In all cases, the X-ray in-

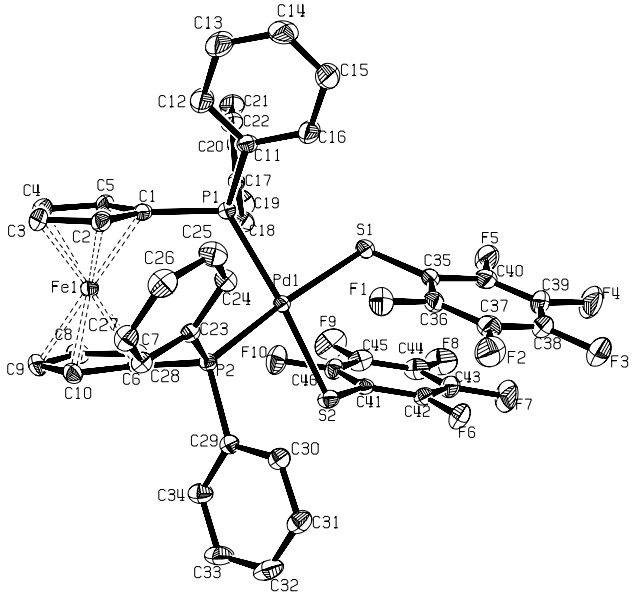

Fig. 1. An ORTEP representation of the structure of $[Pd(dppf)(SC_6F_5)_2]$ (**1**) at 50% probability showing the atom labeling scheme.

tensity data were measured at 291 K on a Bruker SMART APEX CCD-based X-ray diffractometer system equipped with a Mo-target X-ray tube ($\lambda = 0.71073$ Å). The detector was placed at a distance of 4.837 cm from the crystals in all cases. A total of 1800 frames were collected with a scan width of 0.3° in ω and an exposure time of 10 s/frame. The frames were integrated with the Bruker SAINT software package [15] using a narrow-frame integration algorithm. The integration of the data was done using a monoclinic unit cell in all cases to yield a total of 34 845, 33 676, 16 600, 64 554 and 7518 reflections for **1**, **2**, **3**, **4** and **5**, respectively, to a maximum 2θ angle of 50.00° (0.93 Å resolution), of which 7528 (**1**), 7311 (**2**), 3677 (**3**), 14 025 (**4**) and 7115 (**5**) were independent. Analysis of the data showed in all cases negligible decays during data collections. The structures were solved by Patterson method using SHELXS-97 [16] program. The remaining atoms were located via a few cycles of least squares refinements and difference Fourier maps, using the space group $P2_1/n$ with $Z = 4$ for **1**, **2**, **4** and **5** and $C2/c$ with $Z = 4$ for **3**. Hydrogen atoms were input at calculated positions, and allowed to ride on the

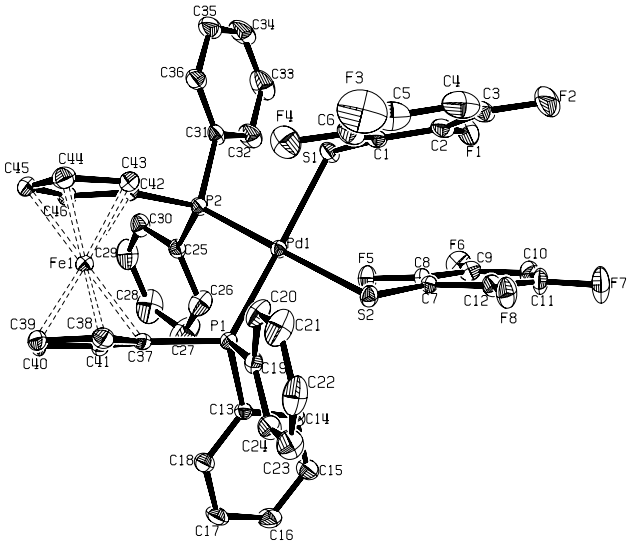

Fig. 2. An ORTEP representation of the structure of [Pd(dppf)(SC_6F_4-4-H)$_2$] (**2**) at 50% probability showing the atom labeling scheme.

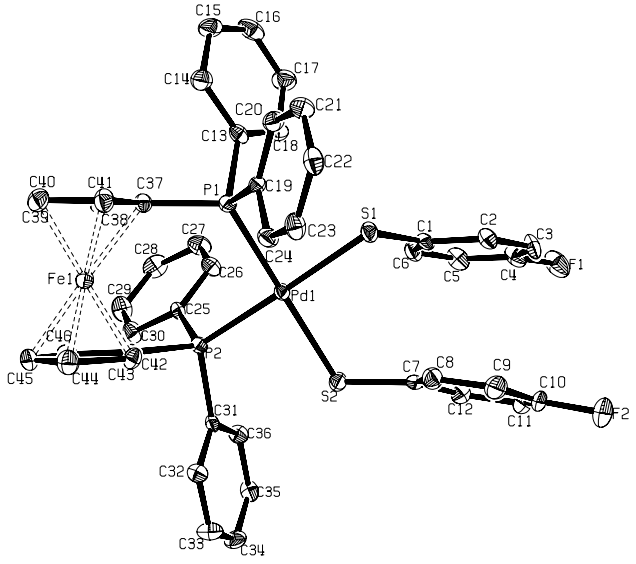

Fig. 4. An ORTEP representation of the structure of [Pd(dppf)(SC_6H_4-4-F)$_2$] (**4**) at 50% probability showing the atom labeling scheme.

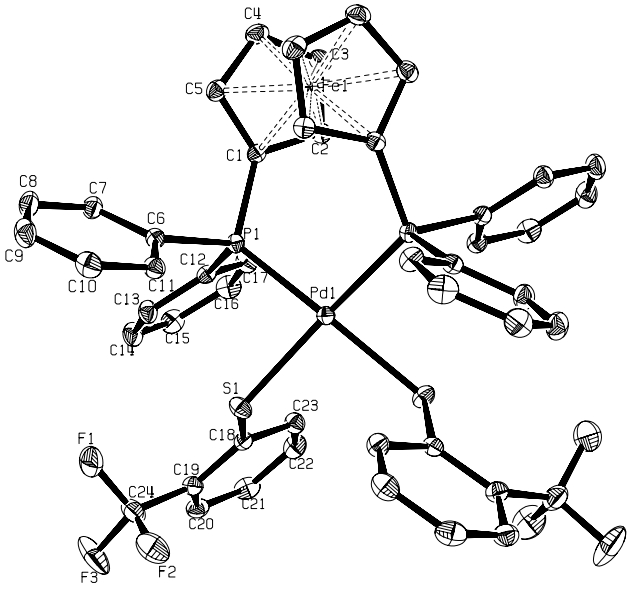

Fig. 3. An ORTEP representation of the structure of [Pd(dppf)(SC_6H_4-2-CF_3)$_2$] (**3**) at 50% probability showing the atom labeling scheme.

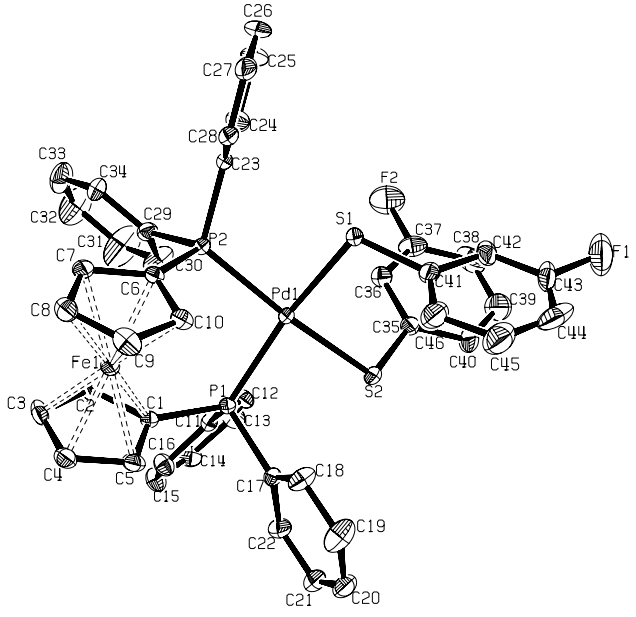

Fig. 5. An ORTEP representation of the structure of [Pd(dppf)(SC_6H_4-3-F)$_2$] (**4**) at 50% probability showing the atom labeling scheme.

atoms to which they are attached. Thermal parameters were refined for hydrogen atoms on the phenyl groups using a $U_{eq} = 1.2$ Å to precedent atom in all cases. For all complexes, the final cycle of refinement was carried out on all non-zero data using SHELXL-97 [16] and anisotropic thermal parameters for all non-hydrogen atoms. The details of the structure determinations are given in Table 1 and selected bond lengths (Å) and angles (°) are given in Table 2, respectively. The numbering of the atoms is shown in Figs. 1–5, respectively, (ORTEP) [17].

4. Supplementary material

Supplementary data for complexes **1**, **2**, **3**, **4** and **5** have been deposited at the Cambridge Crystallographic Data Centre. Copies of this information are available free of charge on request from The Director, CCDC, 12 Union Road, Cambridge, CB2 1EZ, UK (fax: +44-1223-336033; e-mail: deposit@ccdc.cam.ac.uk or www: http://www.ccdc.cam.ac.uk) quoting the deposition numbers CCDC 227072–227076.

Acknowledgements

C.H.-A and V.G.-B thank CONACYT for financial support. We thank Chem. Eng. Luis Velasco Ibarra, M.Sc. Francisco Javier Pérez Flores, QFB. Ma del Rocío Patiño and Ma. de las Nieves Zavala for their invaluable help in the running of the FAB^+-Mass, IR and $^{19}F\{^1H\}$ spectra, respectively. The support of this research by CONACYT (J41206-Q) is gratefully acknowledged.

References

[1] J.J. Bishop, A. Davidson, M.L. Katcher, D.W. Lichtenberg, R.E. Merril, J.C. Smart, J. Organomet. Chem. 27 (1971) 241.
[2] G. Bandoli, A. Dolmella, Coord. Chem. Rev. 209 (2000) 261.
[3] K.S. Gan, T.S.A. Hor, in: A. Togni, T. Hayashi (Eds.), Ferrocenes, Weinheim, VCH, 1995.
[4] T. Colacot, J. Platinum. Met. Rev. 45 (2001) 22 (references therein).
[5] T. Colacot, J. Chem. Rev. 103 (2003) 3101 (references therein).
[6] (a) L.L. Maisela, A.M. Crouch, J. Darkwa, I.A. Guzei, Polyhedron 20 (2001) 3189;
(b) O. Crespo, F. Canales, M.C. Gimeno, P.G. Jones, A. Laguna, Organometallics 18 (1999) 3142;
(c) D-Y Noh, E-M Seo, H-J Lee, H-Y Jang, M-G Choi, Y.H. Kim, J. Hong, Polyhedron 20 (2001) 1939;
(d) V.D. de Castro, G.M. de Lima, A.O. Porto, H.G.L. Siebald, J.D. de Souza Filho, J.D. Ardisson, J.D. Ayala, G. Bombieri, Polyhedron 23 (2004) 63;
(e) T.F. Baumann, J.W. Sibert, M.M. Olmstead, A.G.M. Barrett, B.M. Hoffman, J. Am. Chem. Soc. 116 (1994) 2639.
[7] J.R. Dilworth, J. Hu, Adv. Inorg. Chem. 40 (1993) 411.
[8] (a) D. Morales-Morales, R. Redón, Y. Zheng, J.R. Dilworth, Inorg. Chim. Acta 328 (2002) 39;
(b) D. Morales-Morales, C. Grause, K. Kasaoka, R. Redón, R.E. Cramer, C.M. Jensen, Inorg. Chim. Acta 300–302 (2000) 958;
(c) D. Morales-Morales, R. Redón, C. Yung, C.M. Jensen, Chem. Commun. 1619 (2000);
(d) D. Morales-Morales, R. Redón, Z. Wang, D.W. Lee, C. Yung, K. Magnuson, C.M. Jensen, Can. J. Chem. 79 (2001) 823;
(e) D. Morales-Morales, R.E. Cramer, C.M. Jensen, J. Organomet. Chem. 654 (2002) 44;
(f) X. Gu, W. Chen, D. Morales-Morales, C.M. Jensen, J. Mol. Catal. A 189 (2002) 119;
(g) J.R. Dilworth, P. Arnold, D. Morales, Y.L. Wong, Y. Zheng, The chemistry and applications of complexes with sulphur ligands, in: Modern Coordination Chemistry. The Legacy of Joseph Chatt, Royal Society of Chemistry, Cambridge, UK, 2002, p. 217;
(h) D. Morales-Morales, S. Rodríguez-Morales, J.R. Dilworth, A. Sousa-Pedrares, Y. Zheng, Inorg. Chim. Acta 332 (2002) 101;
(i) V. Gómez-Benítez, S. Hernández-Ortega, D. Morales-Morales, Inorg. Chim. Acta 346 (2003) 256.
[9] D. Cruz-Garritz, J.A. Chamizo, M. Cruz, H. Torrens, Rev. Soc. Quim. Mex. 33 (1989) 18.
[10] (a) L.S. Reddy, A. Nangia, V.M. Lynch, Crystallogr. Growth Des. 4 (2004) 89;
(b) D.B. Fox, R. Liantonio, P. Metrangolo, T. Pilati, G. Resnati, J. Fluoresc. Chem. 125 (2004) 271.
[11] T. Hayashi, M. Konishi, Y. Kobori, M. Kumada, T. Higuchi, K. Hirotsu, J. Am. Chem. Soc. 106 (1984) 158.
[12] M. Ogasawara, K. Yoshida, T. Hayashi, Organometallics 19 (2000) 1567.
[13] D. Drew, J.R. Doyle, Inorg. Synth. 28 (1990) 348.
[14] M.E. Peach, Can. J. Chem. 46 (1968) 2699.
[15] A.X.S. Bruker, SAINT Software Reference Manual, Madison, WI, 1998.
[16] G.M. Sheldrick, SHELXTL NT Version 6.10, Program for Solution and Refinement of Crystal Structures, University of Göttingen, Germany, 2000.
[17] L.J. Farrugia, ORTEP-3 for Windows: J. Appl. Crystallogr. 30 (1997) 565.